

# An Ultrasound-Based Imaging Method for Visualizing Patterns of Action Potential Propagation in the Heart

Niels F Otani, Rupinder Singh, Robert F Gilmour, Jr

Cornell University, Ithaca, NY, USA

## Abstract

*An understanding of the patterns and characteristics of action potential propagation in the heart is crucial for the development of advanced methods for treating dangerous and lethal cardiac rhythm disorders. Unfortunately, visualization of these action potentials with existing methods, especially deep with the walls of the heart, has been problematic. We have been developing a new method whereby these patterns can be seen. The method calculates the locations of action potentials from the deformations they produce, as recorded in ultrasound images. An important step in developing an appropriate algorithm is to determine whether there exists a local function of the mechanical strains that marks the locations of the action potentials, or whether a fully three-dimensional inverse calculation must be performed. To study this question, we have examined the properties of deformations produced by action potentials propagating in: a 1-D fiber, an axisymmetric shell model of the heart and a 3-D model of a cube of cardiac tissue. The models and theory combine to show that incremental strain is a good marker of the action potentials wavefronts when the system and wave are essentially one-dimensional in nature. In contrast, higher dimensional structure in either the wave or the medium in which it travels produces an incremental strain field that extends out away from the wave. We conclude that determination of action potential locations will likely require a more complex calculation when wave propagation is not fundamentally one-dimensional.*

## 1. Introduction

At present, we do not have a fully 3-D method for visualizing action potential propagation in the heart. This limitation has prevented us from fully understanding the dynamics of various arrhythmias in the heart, especially ventricular tachycardia and ventricular fibrillation. Even such entities as spiral wave reentry and scroll waves, commonly used in the description of these arrhythmias, have not been clearly visualized in the 3-D heart.

In this paper, we describe our ongoing efforts to develop a new, ultrasound-based imaging method that we believe will allow visualization of these 3-D action potential propagation patterns. The method may conveniently be described as being composed of a series of steps. First, a series of 3-D images of the heart are taken using a 3-D ultrasound imaging device. Second, a speckle-tracking algorithm is applied to these images to determine the displacements of an array of points in the heart. Third, the force balance equations are used to calculate the action-potential-induced active stresses that must have been present to produce the observed deformations. Fourth, the locations of these active stresses are used to infer the location of the action potentials that produced them. Each of these steps is potentially difficult when put into the context of the role each plays in this visualization method. For example, the last step probably can only be accomplished in some approximate sense, because there does not exist a one-to-one relationship between the membrane potential and the action-potential-induced active stress.

In our recent studies of the third step, that is, the conversion of tissue deformation into active stress [1], we have demonstrated that, while this problem is in general underdetermined, it is overdetermined in the case of the heart, because only one component of the nine-component active stress tensor is nonzero—that associated with stress along the local fiber direction. This reduces the number of quantities we are solving for by a factor of 6 (since there are in general six independent components in a symmetric second-order tensor). We then have the luxury of not only just solving for these stresses, but solving for them in a least-squares sense using the extra equations, which will tend to reduce the effect of measurement errors in the deformations and parameters of the model.

Others have taken a similar approach. In particular, Konofagou et al (e.g., [2]), have extracted the incremental strain (essentially, the time derivative of the strain) from ultrasound images, and used it to infer the location and propagation of the electromechanical wave that is associated with the action potential wave.

In this paper, we examine an important issue associated with this third step; namely, the circumstances un-

der which a measure such as the incremental strain can provide localized information about presence of an action potential. Certainly, if this is possible, then it would be desirable, since the obvious alternative would be to solve the full, spatially 3-D problem, which would require time-consuming and computationally expensive matrix inversions.

## 2. 1-D fiber model

To see why the incremental strain might be a good marker for the action potential wavefront, we look briefly at a one-dimensional fiber model. As shown in Fig. 1, an action potential initiated in the center of a fixed-length fiber and propagating in both directions creates a region of compression in the center of the fiber and regions of stretch at both ends. Thus, as either wavefront passes by any given point, the strain switches from positive to negative, implying the time derivative of the strain (the incremental strain) is negative. We also note that the degree of stretch and compression on either side of the wavefronts changes slowly as the waves propagate, to maintain the fixed-length boundary conditions.

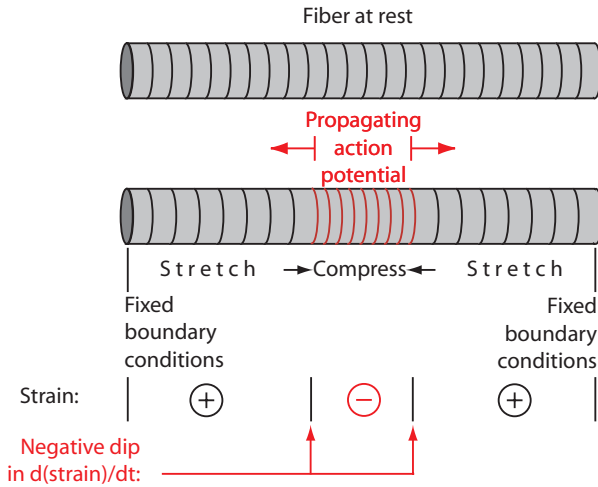


Figure 1. Pattern of deformation produced by two action potential waves propagating from the center of a one-dimensional fiber, assuming both ends of the fiber are fixed.

The pattern of incremental strain will therefore be as shown schematically in Fig. 2. The action potential wavefronts are “marked” with negative dips in the incremental strain profile as they travel through a relatively low-amplitude background of positive incremental strain. A similar statement can be made in the case of free endpoint boundary conditions, except that, in that case, the background incremental strain in which the negative dips travel is just the zero-function.

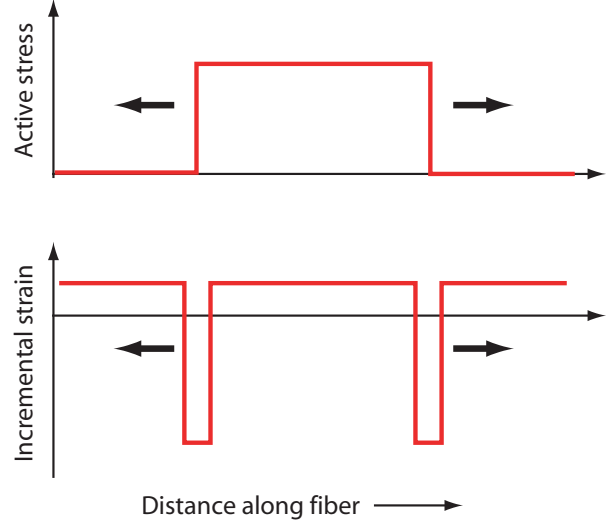


Figure 2. Negative dips in the incremental strains mark the locations of action potential wavefronts propagating in a 1-D fiber.

We can readily see these characteristics in the equations governing the 1-D fiber. If the force balance equation for the fiber is differentiated with respect to time, we obtain,

$$\frac{\partial^2 \xi}{\partial t \partial x} = \frac{1}{Y} \left[ \frac{d}{dt} \left( \frac{1}{L} \int_0^L t_{act}(x', t) dx' \right) - \frac{\partial t_{act}}{\partial t} \right] \quad (1)$$

Here,  $\xi(x, t)$  is the displacement at location  $x$  on the fiber, at time  $t$ ,  $Y$  is Young’s modulus,  $L$  is the length of the fiber, and  $t_{act}$  is the active stress. Thus, the incremental strain (the term on the left) equals a background term that only depends on  $t$  (first term on the right), and a negative dip (second term on the right) when the active stress increases from 0 in the wavefront.

## 3. Axisymmetric shell model

We also conducted a computer simulation of the heart represented simplistically as an axisymmetric thin-shell model. The heart’s shape was created by revolving a function  $R(Z)$  chosen to mimic the shape of a heart around the  $Z$ -axis. The force balance equations were then transformed to the curvilinear coordinate system  $(n, \theta, s)$ , where  $n$  measures normal distance from the surface of the shell,  $\theta$  is the azimuthal angle, and  $s$  is a measure of path length along the function  $R(Z)$ . When an action potential is launched from one end of the shell, a pattern of incremental strain as shown in Fig. 3 results. As in the 1-D fiber case, the leading edge of the action potential is marked by a strong band of incremental strain.

Analysis of the equations for this case also bears a similarity to the 1-D fiber. When constant volume is assumed

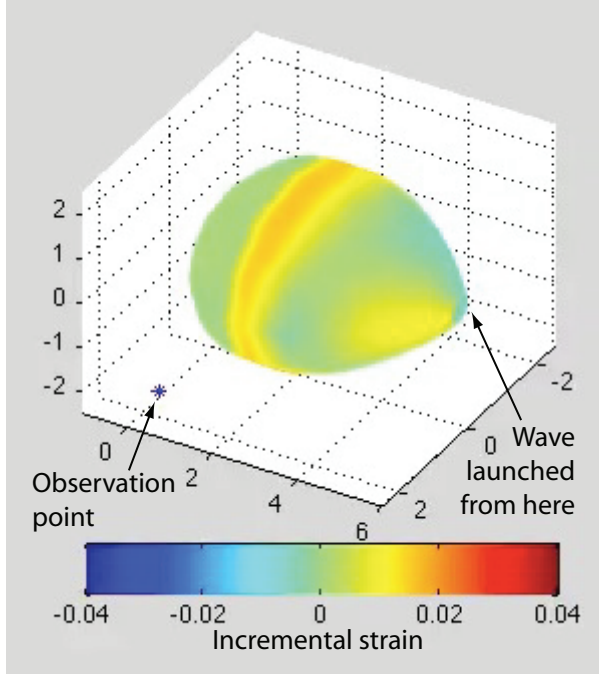


Figure 3. Colormap of the incremental strains produced in an axisymmetric shell model of the heart by an action potential propagating from one end of the shell. The color indicates the degree of incremental strain along the line-of-sight direction seen from the observation point indicated.

inside the shell (e.g., when the valves are all closed in the heart), analogous to the fixed endpoint boundary conditions in 1-D, we find that the incremental strain in the  $s$  direction is,

$$\frac{\partial^2 \delta s}{\partial t \partial s} = \frac{1}{Y} \left( \frac{R\sqrt{1+R'^2}}{2a} \frac{d\delta p_b}{dt} - \frac{\partial t_{act}^{ss}}{\partial t} \right) \quad (2)$$

with a similar equation for the azimuthal incremental strain. Here  $\delta s$  is the displacement along the  $s$  direction,  $a$  is the thickness of the shell, assumed to be small,  $\delta p_b$  is the change in the pressure of the blood assumed to fill the volume, and  $t_{act}^{ss}$  is the active stress in the  $s$  direction. We note the similarity to Eq. (1). The first term on the right-hand side is again a “background” profile, a purely geometric factor  $R\sqrt{1+R'^2}/2a$  that only depends on  $s$  only, multiplied by a purely time-dependent function  $d\delta p_b/dt$  that serves as its amplitude. The second term of the right-hand side again produces a negative dip when the active stress  $t_{act}^{ss}$  suddenly increases, as occurs in an action potential wavefront.

#### 4. 3-D Green’s function response

The two preceding examples are essentially one-dimensional with  $x$  and  $s$ , respectively, serving as the only

nontrivial spatial variables. Suppose now that an infinitesimally small volume within a three-dimensional volume of tissue of infinite extent is subject to an active stress in the  $Z$  direction of magnitude  $t_0$  per unit volume. It has been shown (e.g., in [1]) that, if the point of active stress is at the origin, then the resulting tissue displacements in the  $Z$  direction are given by,

$$\delta Z(r, \theta, \phi) = \frac{1}{r^2} \frac{t_0}{4\sqrt{2\pi}Y} \cos \theta (1 - 3 \cos^2 \theta) \quad (3)$$

with a similar equation for the displacements in the  $R$  direction. The resulting strain patterns, being derivatives of these displacements, have similarly complex spatial structures. We also note that, since these displacements fall off with distance as  $1/r^2$ , the strains will fall off as  $1/r^3$ , and are therefore not localized to the point of active stress causing them. It is therefore reasonable to conclude that incremental stresses will also not be localized.

#### 5. 3-D cube model

It appears that plane-wave action potentials that are propagating in systems that are essentially 1-D in nature will be well-marked by the incremental strains they produce. However, inclusion of 3-D effects may be problematic. To check this assertion, we ran computer simulations using a 3-D model of a cube of heart tissue, which was described in detail in [1]. Briefly, the simulation employs a 3-D finite element model of the force balance equations including incompressibility with free boundary conditions. The model uses the Nash-Hunter characterization of the stress-strain relationship [3] and thus allows for the anisotropy associated with the local fiber direction. The model also allows the fiber orientation within the cube to be a function of position.

When a plane wave of constant active stress is allowed to propagate through the cube in the  $+x$  direction, deformations as shown in Fig. 4 appear. Figures 4(a) and (b) show the case of uniform fiber orientation, with all the fibers throughout the cube pointing in the  $x$ -direction. We observe that, for this case, the incremental strain takes the form of a negative dip confined to the plane occupied by the wavefront at  $x = 4$ .

In contrast, when a rotation in direction is introduced, as in Figs. 4(c) and (d), the pattern of the incremental strain is not longer confined to the plane-wave wavefront, but instead “radiates” both ahead and behind it. Thus, even this relatively mild 3-D feature delocalizes the incremental strain relative to the wavefront. We note, however, that this extended pattern of incremental strains does appear to move with the wavefront, when the series of figures like that shown in Fig. 4(d) is displayed as a movie.

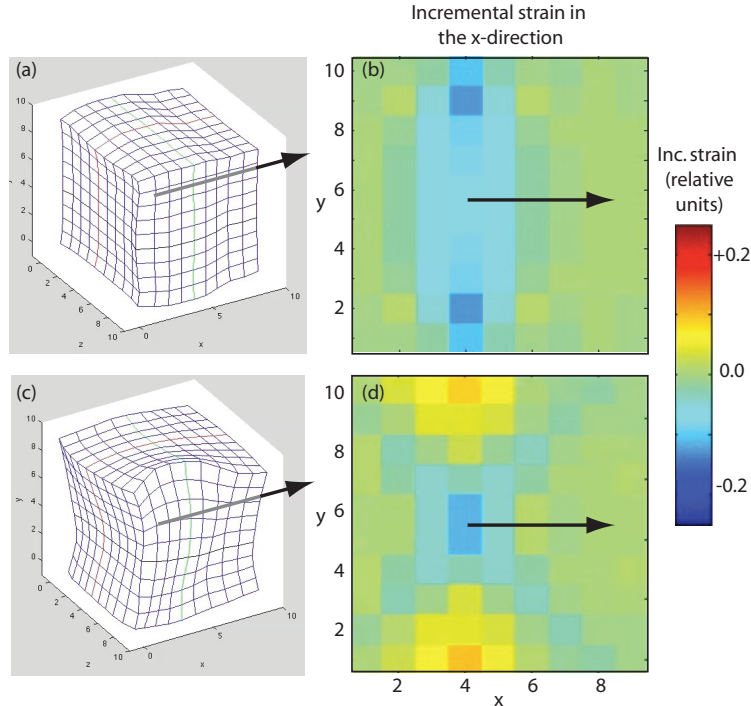


Figure 4. For the case of uniform fiber orientation in the  $x$ -direction throughout a cube model of cardiac tissue: (a) shows the deformation of a cube during the propagation of a plane-wave action potential propagating in the direction of the arrow. (b) shows a colormap of the incremental strains in a planar cross-section of the cube located at  $z = 5$ . (c) and (d) show the deformations and incremental strains for the case of fibers whose orientation rotates from the  $z$  direction at the top of the cube, through  $x$  direction in the middle of the cube, continuing around to the  $z$  direction again at the bottom of the cube. The wavefront of the action potential is located at  $x = 4$  for both of the cases shown.

## 6. Conclusions

We have been investigating the possibility that the mechanical deformations produced by action potentials propagating through the heart, as imaged by ultrasound, may be used to track these action potentials. A negative dip in the incremental strain is found to be a good marker for the action potential wavefront in a 1-D fiber, and also in an axisymmetric fluid-filled, thin-walled vessel, when the wave respects the axisymmetry of the vessel. However, incremental strains are not localized to the action potential in general 3-D geometry. We can, of course, solve for the active stresses by solving the full 3-D inverse problem. However, this procedure is potentially time-consuming, and requires knowledge of the boundary conditions, etc. There are two points of optimism moving forwards. First, while, the incremental strains are not confined to the wavefront, they do fall off as  $1/r^3$  with distance, providing some degree of localization. Second, since the pattern did not change appreciably as the wave propagated, it may be possible to “deconvolve” the pattern back to the wavefront that is producing it. Thus, a method that falls somewhere between the direct marking of wavefronts using incremen-

tal strain and solving the full 3-D inverse problem may be plausible.

## References

- [1] Otani NF, Luther S, Singh R, Gilmour Jr RF. Transmural ultrasound-based visualization of patterns of action potential wave propagation in cardiac tissue. *Ann of Biomed Eng* 2010;38:3112–23.
- [2] Provost J, Gurev V, Trayanova N, Konofagou EE. Mapping of cardiac electrical activation with electromechanical wave imaging: an in silico-in vivo reciprocity study. *Heart Rhythm* 2011;8:752–9.
- [3] Nash MP, Hunter PJ. Computational mechanics of the heart. *J Elasticity* 2000;61:113–141.

Address for correspondence:

Niels F. Otani  
 Dept. of Biomedical Science  
 Cornell University  
 Ithaca, NY 14853 USA  
 E-mail address: nfo@cornell.edu